

Distribution and air-sea exchange of Nitrous oxide in the Coastal Bay of Bengal during peak discharge period (southwest monsoon)

G.D. Rao, V.D. Rao and V.V.S.S. Sarma*

CSIR-National Institute of Oceanography, Regional Centre, 176 Lawson's Bay Colony, Visakhapatnam – 530 017, India.

*Corresponding author (sarmav@nio.org)

Abstract

In order to examine the impact of river discharge from the Indian subcontinent on the concentration and air sea exchange of nitrous oxide (N_2O) a study was conducted during peak discharge period in the coastal Bay of Bengal. The study revealed that freshwater discharge exerts a dominant control on the N_2O cycling in the surface waters of the coastal Bay of Bengal. The surface concentration of N_2O in the southwestern (SW) coastal Bay of Bengal was high (7.4 ± 1.6 nM) and supersaturated ($126 \pm 27\%$) whereas contrasting trend was found in the northwestern (NW) region (4.9 ± 0.3 nM and $81 \pm 6\%$). Such spatial differences in N_2O concentration and saturation were resulted from variable characteristics of the discharged waters, and vertical stratification. The NW region of the coastal Bay of Bengal was under the influence of the discharge from the Ganges River having N_2O below the saturation in the estuary ($82 \pm 5\%$) while the SW region was under the influence of peninsular river discharges that were super-saturated ($187 \pm 29\%$). The low N_2O concentration at NW region was resulted from low concentrations in the source water (Ganges) as these waters were formed by melting of Himalayan glacier where low ammonium concentrations were observed due to less human settlement resulting in lower nitrification rates. Higher concentration of N_2O in the SW region was attributed to the discharge from monsoonal rivers containing high N_2O concentrations, high nitrification rates and mild coastal upwelling. The sea-to-air fluxes of N_2O suggest that NW region is a sink for atmospheric N_2O due to discharge of under saturated water from Ganges and strong stratification while SW region is a source caused by coastal upwelling and discharge of highly saturated water from monsoonal rivers.

1. Introduction

Nitrous oxide (N_2O) is an important greenhouse gas having very long residence time in the atmosphere (100-150 years) compared to other green house gases. N_2O is involved in generating stratospheric NO, which contribute to the net destruction of stratospheric ozone (Crutzen, 1970; Nevison and Holland, 1997). The atmospheric mixing ratio of the N_2O (325 ppbv) is smaller than that of carbon dioxide (CO_2 ; 395 ppmv; <http://www.esrl.noaa.gov/gmd/>), by ~ 1000 times, however, the greenhouse potential of N_2O is ~ 300 times higher than that of carbon dioxide (CO_2) (Forster et al., 2007). The radiative forcing, due to increase in greenhouse gas concentrations from the pre-industrial (1750 to 2011) is estimated to be $+2.839 \text{ Wm}^{-2}$ (comprising CO_2 (1.817 Wm^{-2}), CH_4 (0.506 Wm^{-2}), N_2O (0.178 Wm^{-2}) and halocarbons (0.338 Wm^{-2})), with an uncertainty of 10%. Intensification of fossil fuel combustion and nitrogenous fertilizer application since the pre-industrial era has increased global emission of N_2O (Bange et al., 2010; Suntharalingam et al., 2012). The N_2O concentration in the atmosphere is increasing steadily, ca $0.2\text{-}0.3\% \text{ y}^{-1}$ on average that raises concerns about future global climate change (Khalil et al., 1992; Houghton et al., 2001; Doney et al., 2007; Duce et al., 2008).

N_2O can be formed through processes naturally as well as by anthropogenic activities (Suntharalingam et al., 2012). N_2O is formed under both reductive and oxidative conditions by bacteria during denitrification of nitrate (Knowles et al., 1996) and nitrification of ammonium ion (Yoh et al., 1998) in the marine environment. Denitrification occurs mainly in the suboxic environment and nitrification in the oxygen rich environment such as the well ventilated surface (Codispoti et al., 2001; Naqvi et al., 2000; 2010). The atmospheric budget of N_2O is greatly influenced by its production in the ocean and exchange across the air-sea interface as the oceans are estimated to account for at least one-third ($1.2\text{-}6.8 \text{ Tg N}_2\text{O y}^{-1}$) of N_2O inputs to the atmosphere from all natural sources ($\sim 11 \text{ Tg N}_2\text{O y}^{-1}$; Nevison et al., 1995; Prather et al., 2001; Suntharalingam and Sarmiento, 2000; Ishijima et al., 2010). The recent IPCC synthesis report suggests that flux of N_2O from the rivers, estuaries and coastal waters represents about 22% of the total anthropogenic N_2O source and about 10% of the total source (<http://www.ipcc.ch/>). On the other hand, the natural sources from the open ocean accounts 35% of the total natural source and about 21% of all sources (natural and anthropogenic). However, these estimates carry significant amount of uncertainties due to lack of systematic data from several regions. Bange et al. (1996) noticed that coastal water contributes up to 60% to the total marine emissions. However, N_2O emissions are not uniformly distributed over the ocean surface as tropical upwelling zones containing

oxygen deficient waters make a disproportionately large contribution (Codispoti and Christensen, 1985; Suntharalingam et al., 2000; Codispoti et al., 2001). N₂O cycling mechanisms display sensitivity to the variations in dissolved oxygen concentration and higher yields are noted at low oxygen levels and ascribed to alternate pathways such as enhanced nitrification, denitrification and interactions between the two (Yoshida et al., 1989; Copispoti et al., 2001; Naqvi et al., 2000). In addition to this, denitrification that occurs at low dissolved oxygen concentration, acts as sink for N₂O in the water column (Codispoti et al., 2001; Naqvi et al., 2000).

Based on reported data for the European coastal areas (i.e. Arctic Ocean, Baltic Sea, North Sea, northeastern Atlantic Ocean, Mediterranean Sea, and Black Sea), Bange (2006) reassessed dissolved concentrations and atmospheric emissions of N₂O. Maximum N₂O saturations were found in estuarine systems, whereas the shelf waters, which are not influenced by freshwater plumes, are close to equilibrium with the atmosphere. More recently Barnes and Upstill-Goddard (2011) estimated air-sea exchange of N₂O from the UK estuaries and estimated that the mean fluxes from the European estuaries to be 2.7 μmol N₂O m⁻² d⁻¹ from the. They concluded that the water column nitrification is the major source of N₂O in the European estuaries. This implies that N₂O is mainly sourced from the estuarine systems.

The northeastern Indian Ocean (Bay of Bengal) receives excessive precipitation over evaporation. It also receives a huge amount of freshwater ($1.6 \times 10^{12} \text{ m}^3 \text{ y}^{-1}$; UNESCO, 1979) from the major rivers such as Ganges ($0.44 \times 10^{12} \text{ m}^3 \text{ y}^{-1}$), Godavari ($0.11 \times 10^{12} \text{ m}^3 \text{ y}^{-1}$), Krishna ($0.07 \times 10^{12} \text{ m}^3 \text{ y}^{-1}$) and Mahanadi ($0.06 \times 10^{12} \text{ m}^3 \text{ y}^{-1}$; Kumar et al., 2005) etc. Both precipitation and river discharge peaks during southwest (SW) monsoon (June – September). Very few observations have been carried out so far on the distribution of N₂O in the atmosphere and waters in the Bay of Bengal. Naqvi et al. (1994) measured along the west coastal Bay of Bengal during March-April 1991 whereas Hashimoto et al. (1998) in the central Bay of Bengal during February 1995 and 1996. Their study revealed that surface N₂O saturation and atmospheric fluxes ranged from 70.6 to 253% (mean 106%), and -70.8 to 175.3 μmol (N₂O) m⁻² d⁻¹ (mean 0.78 μmol m⁻² d⁻¹), respectively. The overall N₂O flux from the Bay of Bengal was estimated to be 0.027-0.077 Tg N yr⁻¹ which is substantially lower than that computed for the Arabian Sea (0.33-0.70 Tg N yr⁻¹; Bange et al., 2001). Lower surface saturations and consequently smaller air-sea fluxes in the Bay of Bengal were attributed to strong stratification caused by the immense river runoff. However, the budget estimates may be biased due to lack of seasonal data.

Recently Sarma et al. (2011) observed record levels of $p\text{CO}_2$ ($>30,000 \mu\text{atm}$) in the largest monsoonal estuary in India, Godavari, during peak discharge period whereas other monsoonal estuaries are also significant source to atmosphere during discharge period (Sarma et al., 2012a). The nutrient levels in the monsoonal rivers were also significantly higher during discharge period (Sarma et al., 2010). The discharge of these nutrients and $p\text{CO}_2$ rich waters to the coastal region has significant impact on coastal biogeochemistry (Sarma et al., 2012b). The characteristics of rivers opening into the Bay of Bengal are influenced by activities of local population, terrain characteristics, industrial activities, and pollution levels etc that are widely variable. No observations have been carried out so far along the east coast of India during peak discharge period to understand how discharges from different rivers influence coastal N_2O fluxes. The aim of this study is to understand the influence of major peninsular rivers along the east coast of India on N_2O concentrations and their fluxes at the air-water interface in the coastal Bay of Bengal during southwest monsoon (SWM)/peak discharge period.

2. Material and methods

2.1. Study area

Samples were collected on board ORV Sagar Nidhi (#SN 42) during 23rd July to 10th August 2010, representing peak SW monsoon and high river discharge period, along the east coast of India covering major rivers such as Krishna (KS, KN transects), Godavari (GS, GN) and Mahanadi (MS, MN) and minor rivers, Vamsadara (VD) and Hyadri (HD) (Fig. 1). Seventy three stations were occupied in 9 transects covering both south (S) and north (N) of riverine mouths of major rivers. Transect V (off Visakhapatnam city) was chosen to represent no discharge location. Samples were collected from coast to ~70-100 kms offshore. Samples were also collected in the estuaries of the rivers Krishna, Godavari, Mahanadi and Ganges during same time of coastal sampling to examine the characteristics of the discharging water into the coastal Bay of Bengal. About 3-5 samples were taken using mechanized boat in the estuaries covering about 10 km from the estuarine mouth to upstream estuary. In order to represent spatial variations along the coastal Bay of Bengal, the data were conveniently divided to represent northwestern (NW) (includes data from VD, HD, MN, and MS transects) and southwestern (SW) region of coastal Bay of Bengal (includes data from KS, KN, GS, GN and V transects).

2.2. Sampling and analyses

2.2.1. *Hydrographic parameters*

Water samples were collected using a Seabird Conductivity-Temperature-Depth (CTD)-rosette system fitted with 5 L Niskin bottles. Analysis for nutrients (nitrate, nitrite, ammonium, phosphate and silicate) and dissolved oxygen (DO) were completed shortly after the collection of samples. DO was estimated by potentiometric method following Carritt and Carpenter (1966) using Tritrinado 835 Metrohm autotitrator. Nutrients were analyzed following standard procedures (Grashoff et al., 1992) using auto analyzer. The analytical precision, expressed as standard deviation, was $\pm 0.07\%$ RSD for DO whereas for nitrate+nitrite, ammonium, phosphate and silicate were ± 0.02 , 0.02 , 0.01 and $0.02 \mu\text{M}$ respectively. A volume of 2 to 5 L of water sample was filtered through GF/F filter (Whatman) and phytoplankton biomass retained on filter was extracted with N, N Dimethyl formamide (DMF) for Chlorophyll-a at 4°C in dark for 12 h, and then analyzed spectrofluorometrically (Varian Eclipse Fluorescence spectrophotometer, USA) following Suzuki and Ishimaru (1990). The analytical precision for Chl-a analysis was $\pm 4\%$. The suspended particulate matter (SPM) was measured based on weight difference of the material retained on $0.22 \mu\text{m}$ pore size polycarbonate filters after passing 1 L of sample. Winds were measured continuously along the ship's cruise track using automated weather station (AWS) installed on the ship at 13.5 m above... River discharge data were obtained from dam authorities of the respective river.

2.2.2. *Measurements of N_2O*

The water samples for N_2O were collected in 60 ml amber colored bottles immediately following the sampling of DO. Samples were poisoned with 0.5 ml of saturated HgCl_2 to prevent microbial activity. The samples were analyzed within 2 hours after collection on board. N_2O dissolved in the water was determined by a multiphase head space equilibration technique (McAuliffe, 1971) coupled with Gas Chromatographic (GC) analysis. Briefly, predetermined volume (25 ml) was equilibrated with equal volume of ultra pure helium in a gas tight syringe by vigorously shaking the syringe at room temperature for 5 minutes using wrist action shaker. After equilibrium, the head space was dried over drierite and then injected through a 5-ml sampling loop into a gas chromatograph (Agilent- 6820, USA) and separated over a chromosorb column (80/100 mesh) at 35°C , and N_2O peak was detected with a ^{63}Ni Electron Capture Detector (ECD). The detector was calibrated at regular intervals using a standard gas

mixture of N₂O (Spectra Gases, USA) diluted to different concentrations so that the dilutions are near to ambient concentration of N₂O. These gases were calibrated against NIST standard reference material. A calibration curve was constructed and a factor has been calculated to estimate the concentration of unknown samples. To check the linearity of the detector with time, one laboratory standard was analyzed three times in a day. The ambient concentration of N₂O were measured by collecting atmospheric gas samples in 60 mL gas tight BD syringes with stop cocks and the samples are directly injected to the GC in the same manner as that of sample headspace. The analytical uncertainty (1σ) for N₂O measurements at any depth was less than ±2%, which was estimated from the analysis of duplicate water samples stored for different periods of time in a refrigerator. The precision of N₂O measurement was always better than 1% (at 1σ level).

2.3. Estimation of N₂O saturation and fluxes

The surface saturation of N₂O was calculated as

$$\text{N}_2\text{O saturation} = \{[\text{N}_2\text{O}]^{\text{meas}} / [\text{N}_2\text{O}]^{\text{equ}}\} \times 100$$

Where $[\text{N}_2\text{O}]^{\text{meas}}$ is measured concentration of N₂O in water column and $[\text{N}_2\text{O}]^{\text{equ}}$ is expected N₂O concentration *at insitu* temperature and salinity. The $[\text{N}_2\text{O}]^{\text{equ}}$ was calculated using *in situ* sea surface temperature (SST) and salinity using solubility coefficients of Weiss and Price (1980). During the cruise, atmospheric N₂O was measured and the mean atmospheric mole fraction of N₂O in air comes to 323±6 ppb (n= 162). This value was used for calculating $[\text{N}_2\text{O}]^{\text{equ}}$ and fluxes.

The magnitude of N₂O flux between the aqueous and gaseous phase was calculated as

$$F(\text{gas}) = k \cdot S_{\text{gas}} [\Delta\text{gas}] \quad (1)$$

Where F (gas) is flux, k is the gas transfer velocity (m d⁻¹), S_{gas} is the solubility coefficient of N₂O (mol m⁻³ atm⁻¹) (Weiss and Price, 1980) and Δgas is the difference of N₂O between water and air.

Gas transfer velocity (k) depends on many factors like, primarily wind speed, temperature, turbulence in atmosphere and water (eg. Liss and Merlivat, 1986; Upstill-Goddard, 2006). Wind speed is probably the most important factor controlling the transfer velocity, and different empirical relationships relating k to wind speed have been proposed in literature (e.g. Wanninkhof, 1992; Nighingale et al., 2000;

Borges et al., 2004). Though wind speed is one of the most important parameter controlling the transfer velocity, there are several environmental variables, such as wave geometry, sea surface roughness, turbulence, wave breaking and bubble formation, rainfall, surfactants, bottom driven turbulence, biology of the sea surface microlayer and bubble ebullition etc. (Upstill-Goddard, 2006). There is no single equation developed to elucidate the influence of all these processes/parameters on transfer velocity. For instance, Borges et al. (2004) measured transfer velocity using closed chamber technique for European estuaries but the same cannot be adapted to other estuaries as these measurements are site specific. In this study, the transfer velocity is computed using parameterizations given by three different studies (Liss and Merlivat, (1986) LM86; Wanninkhof, (1992) (W92), Nightingale et al., (2000) (N2000) and compared them. The flux estimated by these coefficients may provide under-estimates due to not considering influence of some of the above said processes.

The sea-to-air fluxes of N_2O were computed from hourly wind speeds data, obtained from automated weather station (AWS) installed on the ship (Astra Microwave Products Limited, Hyderabad, India) at 13.5 m height from the sea surface. Hourly measured wind speed was averaged to obtain daily mean and was used for transfer velocity calculations. The Schmidt number (Sc) for N_2O , which was calculated from temperature (t) according to the polynomial fit given by Wanninkhof (1992) and u_{10} is the wind speed normalized to a height of 10 m above the sea surface and the same is computed following Thomas et al. (2005).

3. Results and Discussion

3.1. Spatial variations in hydrographic properties

Sea surface temperature (SST) was higher in the NW region (28.7 to 30 ° C) compared to that of SW region (27.5 to 28.5 ° C) (Fig. 2). Up slopping of isotherms were noticed along transects in the SW region from offshore to inshore region suggesting the occurrence of coastal upwelling. The winds along the west coast of Bay of Bengal were blown from southwest direction (Figure not shown) during this period that strongly favors coastal upwelling. The occurrence of mild upwelling along the east coast of India was noticed earlier and found to confine close to the coast (Murty and Varadachari, 1968; Shetye et al., 1991; Gopalakrishna and Sastry, 1985). On the other hand, the upper 20-40 m of water column was relatively warmer along transects in the NW region indicating occurrence of strong stratification (Fig. 2). The surface salinity varied between ~22 and 34 in the study region along the west coastal Bay

of Bengal in the upper 20 to 50 m and relatively lower salinities were observed in the NW compared to SW region (Fig. 3). The occurrence of such low saline water (~ 22) in NW region was caused by huge river discharge by Ganges river ($>0.44 \times 10^{12} \text{ m}^3 \text{ y}^{-1}$) due to melting of glaciers on the Himalayan mountain (Conkright et al., 1994). On the other hand, the SW region was influenced by relatively low discharge from the monsoonal or peninsular rivers such as Godavari River ($\sim 0.11 \times 10^{12} \text{ m}^3 \text{ y}^{-1}$) and Krishna River ($\sim 0.07 \times 10^{12} \text{ m}^3 \text{ y}^{-1}$). Unlike river Ganges, discharge occurs from the monsoonal rivers only during wet period (called monsoon) from June to September when peninsular India receives precipitation (Sarma et al., 2009; 2010). The influence of Ganges discharge decreases towards the south of Vamsadhara River mouth due to mixing with local water and circulation pattern (Sarma et al., 2012b).

The surface dissolved oxygen (DO) concentration and saturation in NW region ($194 \pm 9 \text{ } \mu\text{mol kg}^{-1}$; 95%) was higher than that of in the SW region ($166 \pm 16 \text{ } \mu\text{mol kg}^{-1}$; 82% Fig. 4a). The higher DO concentrations were associated with high Chl-a concentration in the NW (1.5 to 7.0 mg m^{-3}) than in the SW region (0.3 - 5 mg m^{-3} ; Fig. 4b). Such high Chl-a in the NW region was resulted from low suspended matter load (SPM) in the NW ($10.3 \pm 2 \text{ mg l}^{-1}$) than in the SW ($32 \pm 2 \text{ mg l}^{-1}$) region (Fig. 4c). The nitrate and ammonium concentrations in the surface water ranged from below detection limit to 6.2 (Fig. 4d) and below detection limit to $3.4 \text{ } \mu\text{mol kg}^{-1}$ (Fig. 4e) respectively with the highest concentration observed in the SW (mainly off Godavari river estuary, GN) region and then decreased towards the NW region. Similarly phosphate (Fig. 4f) and silicate (figure not shown) also showed lower concentrations in the NW than in the SW region. Due to deeper penetration of light, phytoplankton efficiently utilized nutrients in the NW than in the SW region, that led to increase in their biomass and decrease in nutrient concentrations.

3.2. Variations in N_2O concentration along the west coast of Bay of Bengal and influence of river discharge

Low surface N_2O concentrations and saturation were observed in the NW ($4.9 \pm 0.3 \text{ nM}$; 81%) and increased towards SW region ($7.4 \pm 1.6 \text{ nM}$; 122%) (Fig. 5). The mean concentration of N_2O off river mouths in the coastal region was variable due to different characteristics of discharged water. For example, N_2O concentration off Godavari estuary (GS, GN; $7.7 \pm 2 \text{ nM}$; $129 \pm 36\%$) and Krishna estuary (KS, KN; $7.5 \pm 1.2 \text{ nM}$; $128 \pm 22\%$) were higher than that of found at off Visakhapatnam (V; $7.0 \pm 0.7 \text{ nM}$; $113 \pm 12\%$), where no river discharge occurs, suggesting that N_2O was produced in the estuary and

transported into the coastal water (Table 1 and 2). It was observed that European estuaries were highly saturated with respect to N₂O and postulated that estuaries are the major source of N₂O to the coastal regions (Barnes and Owens, 1999; Bange, 2006; Barnes and Upstill-Goddard, 2011). The concentrations of N₂O and saturation in the coastal Bay of Bengal were consistent with the nearby estuaries. (Table 2). The concentrations of N₂O were significantly higher in the monsoonal estuaries, Mahanadi estuary (6.9-16.8 nM; 11.5±6 nM), Godavari estuary (6.4-15.7 nM; 10.6±1 nM) and Krishna estuary (7.0-12.8 nM; 9.9±4 nM), and the lowest concentration was found in the Ganges estuary (5.3-7.5 nM; 6.3±0.7 nM) suggesting that monsoonal river estuaries contain almost twice as much N₂O concentration than the glacial river estuary (Ganges). The origin of the Ganges is in the Garhwal portion of the western Himalayas and is formed due to melting of Himalayan glacier. The source water of Ganges may contain zero N₂O because the formation of ice is a degassing process. Chen et al. (2012) observed undersaturation of N₂O in the Prydz Bay, Antarctica and was attributed to dilution of sea-ice melt water. In addition to this, the en route of Ganges River is relatively pristine due to less human settlements and therefore less nitrogenous inputs into the river that further reduces nitrification rates. Ganges discharges freshwater through several estuaries into the Bay and only few estuaries such as Hooghly were highly polluted due to existence of one of the major cities in India (Kolkata). The N₂O saturation in the Ganges river varied from 80 to 111% and the higher saturation was observed at Hooghly estuary where high industrial activities (port activities) take place. Excluding these points, which will not represent entire river characteristics, the mean N₂O saturation comes to 82±5% (Table 2). Therefore, the concentration of N₂O and its fluxes to the atmosphere in the coastal region are dependent on the type of river discharge - monsoonal or glacial. Despite high concentration of N₂O in the Mahanadi (11.5±6 nM; 209%), low N₂O concentration were found in the NW region due to dominant discharge from Ganges river (>0.44×10¹² m³ y⁻¹) as the chemical signals of Ganges were preserved through out NW coastal Bay of Bengal. This signal is lost as the water flows further south due to dilution. The strong positive relationship of N₂O saturation with salinity (r²=0.71; p<0.001) indicates that high river runoff and the subsequent spreading of fresh water from Ganges estuary sustained surface circulation that led to low N₂O concentration in NW region (Fig. 5).

The vertical distribution suggests that N₂O concentrations in the upper 100 m were relatively higher in the SW compared to NW region. For instance, the contour of 10 nM N₂O was situated below 50 m in the NW region which has been uplifted to above 20 m in the SW region (Fig. 6). In order to examine the

vertical gradients, the variations in physical and chemical properties at the surface were compared with the same at the depth of 50m and 100m (Fig. 7). The salinity difference between surface and 50m water column depth was small (<0.5 to 1.0) in the SW region whereas it was increased to ~13 towards NW region and this distribution pattern strongly suggests that occurrence of strong stratification in the latter region (Fig. 7a). Similarly high nitrate and ammonium concentrations were found in the surface with increased concentrations at 50m depth in the SW region which were relatively low at the NW region suggesting that low concentrations in the upper 50 m in the latter region (Fig. 7b, c). This was mainly caused by higher biological uptake as evidenced from higher Chl-a in the NW than in the SW region (Fig. 4b). Low ammonium concentrations in the NW region leads to low nitrification and adds less N₂O to the surface waters. Since N₂O in the source waters of NW region were low due to glacial river discharge, prevailing low ammonium concentration further will not enhance its concentration through nitrification. Furthermore strong stratification inhibits N₂O inputs from the subsurface waters. In addition to this The concentration gradient of N₂O between surface and 50 m depth was large in the SW region (~20 nM) whereas it was <10 nM in the NW region. In contrast, N₂O concentrations at 100 m and below did not show large differences between NW and SW regions suggesting that coastal upwelling enhanced N₂O concentrations in the upper 100 m in the latter region (Fig. 7d).

3.3. Variations in N₂O saturation and fluxes at air-water interface

The surface water N₂O saturation ranged from 70.6 to 253% with an average of 106±31% (anomaly (N₂O_{ana}) of +6%). The N₂O saturation was high in the SW region (126±27%; N₂O_{ana}=+26%) compared to NW region (81±6%; N₂O_{ana}=-19%) during SW monsoon. The highest super saturation of 253% (N₂O_{ana}=+153%) was observed off Godavari estuary (Table 1). The super saturation of N₂O in the SW region was driven by coastal upwelling. Naqvi et al. (1994) observed overall super saturation of 125% (N₂O_{ana}=+25%) in the coastal Bay of Bengal during dry period (March-April, 1991) and varied from under-saturation (89%; N₂O_{ana}=-11 %) to super saturation (214%; N₂O_{ana}=+114%) when monsoonal rivers were almost dried up and minimal discharge from the Ganges river. Under saturation of N₂O was attributed to strong stratification resulted by immense river runoff (Naqvi et al., 1994) as it was evidenced from low vertical exchange coefficient (0.16 cm² s⁻¹) at the top of the thermocline in the Bay of Bengal compared to that of the Arabian Sea (0.55 cm² s⁻¹).

The mean saturation anomaly during SW monsoon in the Bay of Bengal (+6.4%) was double to that of the global average anomaly of +3.46% (Nevison et al., 1995). In contrast, the mean saturation anomaly

during February (+19%) and March-April (+25%) were above the global average (6-8 times) in the western and central Bay of Bengal (Naqvi et al., 1994; Hashimoto et al., 1998). Nevertheless, the saturation anomaly in the Bay of Bengal is much smaller than that found in the Arabian Sea (Laws and Owens, 1990; Naqvi and Norohna, 1991). Naqvi et al., (2000) noticed $>+1000\%$ saturation anomaly (up to +8200%) in the coastal Arabian Sea where intense denitrification occurs during SW monsoon. Such high saturation levels in the Arabian Sea were driven by both nitrification and denitrification whereas only former process contributes in the Bay of Bengal (Sarma et al., 2013a,b). On the other hand, Bange (2006) and Barnes and Upstill-Goddard (2011) found that the highest saturation of N_2O was observed in the estuaries and decreased towards coastal regions which is mainly sourced by nitrification process. They further attributed that European coastal regions are net source of N_2O to the atmosphere with the major contribution coming from estuarine/river systems. The N_2O saturation in the monsoonal estuaries, such as Godavari ($208\pm 91\%$; $N_2O_{ana}=+108\%$; $n=5$), Krishna ($166\pm 41\%$; $N_2O_{ana}=+66\%$; $n=3$), and Mahanadi ($209\pm 83\%$; $N_2O_{ana}=+109\%$; $n=5$), were significantly higher than the coastal region while under saturation was noticed in the Ganges River ($82\pm 5\%$; $N_2O_{ana}=-18\%$; $n=6$), excluding the higher values found in the Hooghly port area. Since NW region was dominated by discharge from the Ganges River, the mean N_2O showed under saturation ($81\pm 6\%$; $N_2O_{ana}=-19\%$). Due to huge freshwater discharge from Ganges, strong stratification was developed that inhibited vertical mixing and supply of N_2O from the subsurface layers, where N_2O accumulates due to higher yield of N_2O . On the other hand, over saturation of N_2O was noticed in the SW region ($126\pm 27\%$; $N_2O_{ana}=+26\%$) where volume of discharge from the monsoonal river was small but with higher saturation levels. Therefore, over saturation of N_2O in the SW region of coastal Bay of Bengal was driven by the estuaries, and coastal upwelling.

Nevertheless, the N_2O saturation found in the NW regions (81% ; $N_2O_{ana}=-19\%$) was less than that earlier investigation (89% ; $N_2O_{ana}=-11\%$; Naqvi et al., 1994) due to existing spatial variability and atmospheric conditions. The atmospheric pressure was decreased from 1000 hPa in the SW region to 998 hPa in the NW region associated with enhancement of wind speed from $\sim 16 \text{ m s}^{-1}$ in the SW to $\sim 22 \text{ m s}^{-1}$ (range of $13.1\text{-}25.5 \text{ m s}^{-1}$) in the NW region (Table 1). These atmospheric features suggest formation of cyclonic conditions in the NW region during study period. The sea-to-air flux of N_2O ranged between -27.5 and $+22.8 \mu\text{mol m}^{-2}\text{d}^{-1}$ using LM 86 whereas it was ranged from -54.8 to $+45$ and -41.5 to $31.2 \mu\text{mol m}^{-2} \text{d}^{-1}$ using W92 and N2000 respectively (Table 1). From the average value of sea-

to-air flux of N₂O SW region was found to be source to the atmosphere (14.3 to 28.2 $\mu\text{mol m}^{-2}\text{day}^{-1}$) due to coastal upwelling and discharge of highly saturated water from monsoonal estuaries while NW region acts as sink (-34.6 to -17.9 $\mu\text{mol m}^{-2}\text{day}^{-1}$) resulted from the discharge of undersaturated water from Ganges. Relatively higher fluxes were estimated using the W92 followed by N2000 and LM86 (Table 1). The mean sea-to-air fluxes of N₂O suggest coastal Bay of Bengal acts as a source for atmospheric N₂O (0.78 $\mu\text{mol m}^{-2} \text{d}^{-1}$) during SW monsoon based on W92. Naqvi et al. (1994) observed that the Bay of Bengal acts as a mild source of N₂O during non-monsoon period (March-April; $0.65\pm 2 \mu\text{mol m}^{-2} \text{d}^{-1}$) to the atmosphere using W92 parameterization. By and large Bay of Bengal acts as a mild source of N₂O to the atmosphere.

Acknowledgements

We thank the Director, NIO, Goa, and Scientist – in charge for encouragement and support. This work is a part of the Supra Institutional Project (SIP 1308) funded by Council of Scientific and Industrial Research (CSIR). We appreciate the help of ship's master, officers and crew for their help during sampling and also thank Ministry of Earth Science (MoES) for allotting ship time for this study. We would like to thank two anonymous reviewers for their constructive comments to improve the quality of manuscript. This is NIO contribution number.....

References

- Bange H W, Rapsomanikis S, Andreae MO. Nitrous oxide in Coastal waters. *Global biogeochem Cycle*. 1996;10: 197-207.
- Bange HW, Andreae M O , Lal S, Law C S, Naqvi S W A, Patra P K, Rixen T, Upstill Goddard R C. Nitrous oxide emissions from the Arabian Sea: A synthesis. *Atmos Chem Phys Discuss*. 2001; 1: 167–192.
- Bange HW. Nitrous oxide and Methane in European Coastal waters. *Estuar Coast Shelf Sci*. 2006; 70: 367-374.
- Bange HW, Freing A, Kock A, Loscher C. Marine pathway to nitrous oxide, in *Nitrous oxide and Climate Change*, edited by K.Smith, Earth scan, London .2010; 36-62.
- Bates N, Knap AH, Michaels AF. Contribution of hurricanes to local and global estimates of air-sea exchange of CO₂. *Nature*. 1998; 395: 58-61.

- Barnes J and Upstill Goddard RC. N₂O seasonal distributions and Air Sea exchange in UK estuaries: Implications for the tropospheric N₂O source from European coastal waters. *J Geophys Res.*2011; 116, G01006, doi: 10.1029/2009JG001156.
- Barnes J and Owens N J P. Denitrification and nitrous oxide concentrations in the Humber Estuary, UK, and adjacent coastal zones. *Mar Pollut Bull.*1999; 37(3–7): 247–260, doi: 10.1016/S0025-326X(99)00079-X.
- Benarde MA. *Globalwarming*.pp.John Wiley, Chichester; 1992.
- Borges AV, Delille B, Schiettecatte LS, Gazeau F, Abril G and Frankignoulle M. Gas transfer velocities of CO₂ in three European estuaries (Randers Fjord, Scheldt, and Thames).*Limnol Oceanogr.* 2004; 49(5):1630–1641.
- Carritt D.E. and Carpenter J H. Comparison and evaluation of currently employed modifications of the Winkler method for determining dissolved oxygen in seawater; a NASCO report. *J Mar Res.*1966; 24: 286–318.
- Chen L Q, Zhan L Y, Xu SQ, Zhang JA,Zhang YU,Guojie XU. Multiple processes affecting surface sea water N₂O saturation anomalies in tropical oceans and Prydz Bay, Antratica.*Adv polar Sci.*2012;23:87-94,dio10.3724/SP.J.1085.2012.00087.
- Clark JF, Wanninkhof R, Schlosser P and Simpson H. J. Gas exchange rates in the tidal Hudson River using a dual tracer technique.*Tellus B* .1994; 46(4): 274–285, doi:10.1034/j.1600-0889.1994.t01-2-00003.x.
- Codispoti LA, Christensen J P. Nitrification Denitrification and nitrous oxide cycle in the eastern tropical South Pacific Ocean. *Mar chem.* 1985; 16: 277-300.
- Codispoti L A, Brandes J A, Christensen J P, Devol A H, Naqvi S W A, Paerl H W, Yoshinari T. The oceanic fixed nitrogen and nitrous oxide budgets: Moving targets as we enter the Anthropocene. *Sci Mar.* 2001; 65: 85–105
- Cohen Y, Gordon LI. Nitrous oxide production in the ocean. *J Geaophy Res.* 1979; 84: 347-353.
- Conkright M E, Levitus S, Boyer T P, Bartolocci D M, Luther ME. *Atlas of the Northern Indian Ocean.* Univ of South Florida: St. Petersburg; 1994.p. 36.
- Crutzen P J. The influence of nitrogen oxides on the atmospheric ozone content. *Quarterly Journal Review of the Meteorological Society.* 1970; 96:320-325.
- Doney S et al. Impacts of anthropogenic atmospheric nitrogen and sulfur deposition on ocean acidification and inorganic carbon system. *Pro Natl Acad Sci. USA.* 2007; 104: 14:580-14:585, dio: 10.1073/pnas.0702218104.
- Duce R A, LaRoche J, Altieri K, Arrigo K R et al. Impactsof atmospheric anthropogenic nitrogen on the open ocean, *Science.* 2008; 320: 893–897.

Forster, P, Ramaswamy V, Artaxo P, Bernsten T, Betts R, Fahey D W, et al. Changes in atmospheric constituents and in radiative forcing, in climate change 2007: The Physical Science Basis. Contribution of Working Group I to the Fourth Assessment Report of the Intergovernmental panel on Climate change, edited by S.Solomon et al. Cmbridge UK: Cambridge Univ Press; 2007.p.129-234,

Gopalakrishna VV and Sastry J S. Surface circulation over the shelf off the east coast of India during southwest monsoon. *Indian J Mar Sic.* 1985; 14: 62–65.

Goreau TJ, Kaplan WA, Wofsy SC, McElroy MB, Valois FW, Watson SW. Production of NO₂ and N₂O by nitrifying bacteria at reduced concentrations of oxygen. *Appl. Environ. Microbiol.* 1980; 40: 526-532.

Grashoff K, Ehrhardt M, Kremling . *Methods of Seawater Analysis.* New York: Verlag Chemie; 1992. p.419.

Hasimoto S, Kurita Y, Takasu Y, Otsuki A. Significant difference in vertical distribution of nitrous oxide in the central Bay of Bengal from that in the western area. *Deep Sea Res.* 1998; 45: 301-316.

Houghton JT, Meirafilho LG, Callander BA, Harris N, Kattenberg A, Maskell K. *The science of climate change.* Cambridge: Cambridge university press; 1996.p.572.

Houghton JT, Ding Y, Griggs DJ et al. *The scientific basis Climate change.* Cambridge: Cambridge university press; 2001.p.881.

Ishijima K, Patra PK, Masayuki T, Toshinobu M, Hidekazu M, Yosuke S et al. Stratospheric influence on the seasonal cycle of nitrous oxide in the troposphere as deduced from aircraft observation and model simulation. *J Geophys Res.*2010; 115:D20308, dio: 10.1029/2009JD013322.

Khalil MAK, Rasmussen RA.The global sources of nitrous oxide. *J Geophys Res.*1992; 97: 14651-14660.

Knowles R. Denitrification: Microbiology and Ecology. *Life Support Biosph Sci.* 1996; 3: 31-4.

Law C S, Owens NTP. Significant flux of atmosphere nitrous oxide from northwest Indian Ocean. *Nature.* 1990; 346: 826-828.

Liss PS , Merlivat L. Airsea exchange rates: introduction and synthesis. In P.Baut-Menard (Ed.), *the role of sea-air exchange in geochemical cycling* .Dordrecht: Reidel; 1986. p. 113-127.

McAuliffe C. GC determination of solutes by multiple phase equilibrations. *Chem Tech.* 1971; 1: 46-50.

Milliman J D, Meade R H. World-wide delivery of river sediment to the oceans. *J Geol.* 1983; 91: 1-21.

Murty CS, Varadachari VVR. Upwelling along the east coast of India. *Bull Natl Inst Sic.* 1968; 36: 80–86

Naqvi SWA, Noronha RJ. Nitrous oxide in Arabian Sea. *Deep sea Res.*1991; 38: 871-890.

Naqvi SWA, Jayakumar DA, Nair M, Kumar MD, George MD. Nitrous oxide in the western Bay of Bengal. *Marine chemistry*. 1994; 47: 269-278.

Naqvi SWA, Jayakumar DA, Narvekar PV, Naik H, Sarma VVSS, DSouza W, Joseph S, George MD. Increased marine pollution of N₂O due to intensifying anoxia on the Indian continental shelf. *Nature*.2000; 408: 346-349, doi: 10.1038/35042551.

Naqvi SWA, Bange HW, Farias L, Monteir PMS, Scranton MI, Zhang J. Marine hypoxia/anoxia as a source of CH₄ and N₂O. *Biogeosci*. 2010; 7: 215-2190, doi: 10.5194/bg-7-2159.

Nevison CD, Wiss RF, Erickson JD. Global oceanic emission of nitrous oxide. *J Geophy Res*. 1995; 100:809-820.

Nevison CD, Holland E.A. Re-examination of the impact of anthropogenically fixed nitrogen on atmospheric N₂O and the stratospheric O₃ layer, *J.Geophy.Res*. 1997; 102:519-537.

Nightingale PD, Malin G, Law CS, Watson JA, Liss PS et al. In situ evaluation of Air Sea exchange parameterization using novel conservative and volatile tracers. *Global Biogeochem cycles*.2000; 14:373-387

Prather M, Ehhalt D, Pentener F et al. *Climate Change, The scientific basis*, Cambridge: Cambridge university press; 2001; p.239-287.

Rao C K, Naqvi SWA, Kumar MD, Varaprasad SJD, Jaya Kumar DA, George MD, Singbal SYS.. Hydrochemistry of the Bay of Bengal: Possible reasons for a different water-column cycling of carbon and nitrogen from the Arabian Sea. *Mar Chem*.1994; 47: 279-290.

Sarma VVS.S., Gupta SNM, Babu PVR, Acharyya T, Harikrishnachari N et al. Influence of river discharge on plankton metabolic rates in the tropical monsoon driven Godavari estuary, India. *Estuarine Coastal and Shelf Sci*. 2009; 85: 515-524.

Sarma VVSS, Prasad VR, Kumar BSK, Rajeev K, Devi BMM, Reddy NPC et al. Intra annual variability in nutrients the Godavari estuary India, *Continental shelf Res*. 2010;30: 2005-2014.

Sarma VVSS, Kumar NA, Prasad VR, Venkataramana V, Kumar BSK, Naidu SA et al. High CO₂ emissions from the tropical Godavari estuary (India) associated with monsoon river discharges, *Geophys Res Lett*. 2011; 38:L08601, doi: 10.1029/2011GL046928.

Sarma VVSS, Krishna MS, Rao VD, Viswanadham R, Kumar NA, Kumai R et al. Sources and Sinks of CO₂ in the west coast of Bay of Bengal, *Tellus B*. 2012(a); 64: 10961, doi: 3402/tellusb.v64i0.10961.

Sarma VVSS, Viswanadham R, Rao GD, Kumar BSK, Prasad VR, Naidu SA et al. Carbon dioxide emissions from Indian monsoonal Estuaries. *Geophy Res Lettrs*.2012 (b); 39: doi: 10.1029/2011GL050709

Sarma VVSS, Krishna MS, Viswanadham R, Rao GD, Rao VD et al. Intensified oxygen minimum zone on the western shelf of Bay of Bengal during summer monsoon: influence of river discharge, *J. Oceanogr.*, 2013a; 69: 45-55.

Sarma VVSS, Sridevi B, Maneesha K, Sridevi T, Naidu SA. Et al. Impact of atmospheric and physical forcings on biogeochemical cycling of dissolved oxygen and nutrients in the coastal Bay of Bengal, *J. Oceanogr.*, 2013b, doi:10.1007/s10872-012-0168-y.

Shetye SR, Shenoi SSC, Gouveia AD, Michael GS, Sundar D, Nampoothiri G. Wind-driven coastal upwelling along the western boundary of the Bay of Bengal during the southwest monsoon, *Cont. Shelf. Res.* 1991; 11: 1397–1408.

Shetye SR. The movement and implications of the Ganges- Brahmaputra runoff on entering the Bay of Bengal, *Curr Sci.* 1993; 64: 32–38.

Suzuki R, Ishimaru T. An improved method for the determination of phytoplankton chlorophyll using N, N-dimethylformamide. *J Oceanography.* 1990; 46: 190-194.

Suntharalingam P, Sarmiento JL. Factors governing the oceanic nitrous oxide distribution; simulation with an ocean general circulation model. *Global Biogeochem cycles.* 2000; 14: 429-454.

Suntharalingam P, Buitenhuis E, Quere LC, Dentener F, Nevison C, Butler HJ, Bange HW, Foster G. Quantifying the impact of anthropogenic nitrogen deposition on oceanic nitrous oxide. *Geophys Res Lett.* 2012; 39: L07605, doi: 10.1029/ 2011GL050778, 2012.

Thomas B.R., Kent EC., and Swail, VR. Methods to homogenize wind speeds from ships and buoys. *Int. J. Clim.*, 25, 979-995.

UNESCO. Discharge of Selected Rivers of the World, Paris.1979

Upstill Goddard R C. Air–sea gas exchange in the coastal zone. *Estuarine Coastal Shelf Sci.*2006; 70: 388–404, doi:10.1016/j.ecss.2006.05.043.

Weiss RF. Nitrous oxide in the surface water and marine atmosphere of north Atlantic and Indian Ocean. *Eos Trans Atm Geophys Union.* 1978; 59: 347-359.

Weiss RF, Price BA. Nitrous oxide solubility in water and seawater. *Mar Chem.*1980; 8: 347-359.

Wanninkhof R. Relationship between wind speed and gas exchange over the ocean.

J Geophys Res. 1992; 97: 7373-7382.

Yoh M, Terari H, Saijio Y. A preliminary study on nitrous oxide production through nitrification in Lake Kizaki. *Jap J Liminol.* 1988; 49: 3-6.

Yoshida N, Morimoto H, Hirano M, Koike I, Matsuo S, Wada E, Saino T, Hattori A.

Nitrification rates and N¹⁵ abundances of N₂O and NO₃ in the western North Pacific. *Nature.* 1989;342: 895–897.

Table 1: Mean (\pm SD) of sea surface temperature, salinity, DO, DO saturation, ammonium, N₂O, N₂O saturation, wind speed and flux at water-air interface along the different cruise transects in the coastal Bay of Bengal.

Transect	Temp (°C)	Salinity (PSU)	DO ($\mu\text{mol kg}^{-1}$)	DO _{Sat} (%)	Ammonium ($\mu\text{mol kg}^{-1}$)	N ₂ O (nM)	N ₂ O _{sat} (%)	Wind (m s ⁻¹)	Flux($\mu\text{mole m}^{-2} \text{d}^{-1}$)		
									LM86	W92	N2000
KS	28.3 \pm 0.3	33.1 \pm 1	172 \pm 8	81 \pm 4	1.7 \pm 0.7	8.0 \pm 1.5	137.5 \pm 26	13.1	12.3 \pm 8.6	26.1 \pm 8	18.8 \pm 3.1
KN	27.7 \pm 0.3	33.9 \pm 0.1	153 \pm 18	72 \pm 8	1.9 \pm 0.5	7.0 \pm 0.7	118.9 \pm 12	18.1	13.5 \pm 8.8	25.5 \pm 6.7	19.5 \pm 7.2
GS	28.2 \pm 0.5	33.8 \pm 0.1	171 \pm 6	81 \pm 3	3.5 \pm 1.6	8.1 \pm 2.9	138.7 \pm 50	16.8	22.8 \pm 9.2	45 \pm 5.7	31.2 \pm 9.9
GN	27.4 \pm 0.6	32.2 \pm 0.6	166 \pm 20	80 \pm 9	1.7 \pm 0.4	7.2 \pm 0.7	119.2 \pm 10	16.7	12.3 \pm 6.4	23.7 \pm 6.8	18.2 \pm 9.7
V	29.0 \pm 0.4	33.3 \pm 0.2	173 \pm 12	82 \pm 6	0.2 \pm 0.01	6.7 \pm 0.7	113.1 \pm 12	20.2	10.6 \pm 9.7	20.5 \pm 8.8	15.7 \pm 4.4
VD	29.1 \pm 1.1	29.2 \pm 1.2	187 \pm 7	87 \pm 1	0.8 \pm 0.4	5.4 \pm 0.4	88.2 \pm 5.8	17.2	-7.04 \pm 3.4	-12.3 \pm 6.1	-9.6 \pm 4.7
HD	29.1 \pm 0.3	25.7 \pm 1.6	191 \pm 5	88 \pm 2	0.4 \pm 0.3	4.8 \pm 0.2	78.9 \pm 4.1	17.9	-13.1 \pm 2.7	-25.2 \pm 5.9	-18.1 \pm 3.7
MS	29.7 \pm 0.1	21.7 \pm 0.8	196 \pm 6	99 \pm 6	0.5 \pm 0.21	4.9 \pm 0.3	78.7 \pm 4.7	24.2	-23.9 \pm 5.2	-46.3 \pm 6.2	-34.9 \pm 7.7
MN	29.8 \pm 0.1	23.5 \pm 1.8	202 \pm 13	92 \pm 6	0.4 \pm 0.1	4.8 \pm 0.3	77.3 \pm 4.3	25.5	-27.5 \pm 5.7	-54.8 \pm 4.9	-41.5 \pm 8.7

*LM 86, W92 and N2000 represents the flux calculated using Liss and Merlivat (1986), Wanninkhof (1992) and Nightingale et al (2000) parameterization for transfer velocity respectively.

Table 2: Ranges and mean concentrations of river discharge, salinity, (\pm SD) concentration, saturation and fluxes of N₂O in the estuaries.

Estuary	Mean discharge (10 ¹² m ³ y ⁻¹)	Salinity*	N ₂ O conc* (nM)	Saturation* (%)	Flux (μ mole m ⁻² day ⁻¹)
Krishna	0.07	4.75-5.03 (5.27 \pm 0.6)	7.0-12.8 (9.9 \pm 4)	121-220 (166 \pm 41)	1.2-14.9 (7.4 \pm 6.1)
Godavari	0.11	0.08-0.3 (0.16 \pm 0.1)	6.4-15.7 (10.6 \pm 1)	118-309 (208 \pm 91)	1.1-50.6 (19.3 \pm 14.1)
Mahanadi	0.06	0.06-0.07 (0.07 \pm 0.1)	6.9-16.8 (11.5 \pm 6)	115-379 (209 \pm 83)	0.2-15.6 (11.2 \pm 10.6)
Ganges	0.44	0.56-0.81 (0.71 \pm 0.1)	5.3-7.5 (6.3 \pm 0.7)	78-85 [§] (82 \pm 5)	-0.82-0.3 (-0.25 \pm 0.7)

[§] excluding higher saturation observed in the port region

*mean \pm standard deviation are given in brackets .Flux were calculated using Wanninkhof (1992).

Legend to figures

Figure 1: Sampling locations in the western coastal Bay of Bengal. Isobaths of 250, 500 and 1000m were also shown. Acronyms K, G, VD, HD, M stands for rivers Krishna, Godavari, Vamsadara, Hyadri and Mahanadi whereas N and S attached to the river names represents north and south of the mouth of the estuary respectively.

Figure 2: Vertical distribution of temperature along the transects a) KS, b) KN, c) GS , d) GN, e)V, f) VD, g) HD, h) MS, i) MN. X- Axis shows distance from the coast and Y- Axis shows depth of water the column.

Figure3: Vertical distribution of salinity along the transects a) KS, b) KN, c) GS , d) GN, e)V, f) VD, g) HD, h) MS, i) MN. X- Axis shows distance from the coast and Y- Axis shows depth of water the column

Figure 4: Distribution of a) DO ($\mu\text{mol kg}^{-1}$) b) Chl-a (mg m^{-3}), c) SPM (mg l^{-1}), d) Dissolved nitrate ($\mu\text{mol kg}^{-1}$) e) Dissolved Ammonium ($\mu\text{mol kg}^{-1}$), and f) Dissolved phosphate ($\mu\text{mol kg}^{-1}$) in the west coast of the Bay of Bengal..

Figure 5: Relationship between salinity and N_2O saturation in the coastal Bay of Bengal. The open and closed circles represents NW and SW region respectively.

Figure 6: Vertical distribution of N_2O along the transects a) KS, b) KN, c) GS , d) GN, e) VSP, f) VD, g) HD, h) MS, i) MN. X- Axis shows distance from the coast (km).

Figure 7: Distribution of a) Salinity, b) Nitrate c) Ammonium and d) N_2O in surface (Closed circle), 50 m (square) and 100 m (triangle) water column depth.

Figure 1.

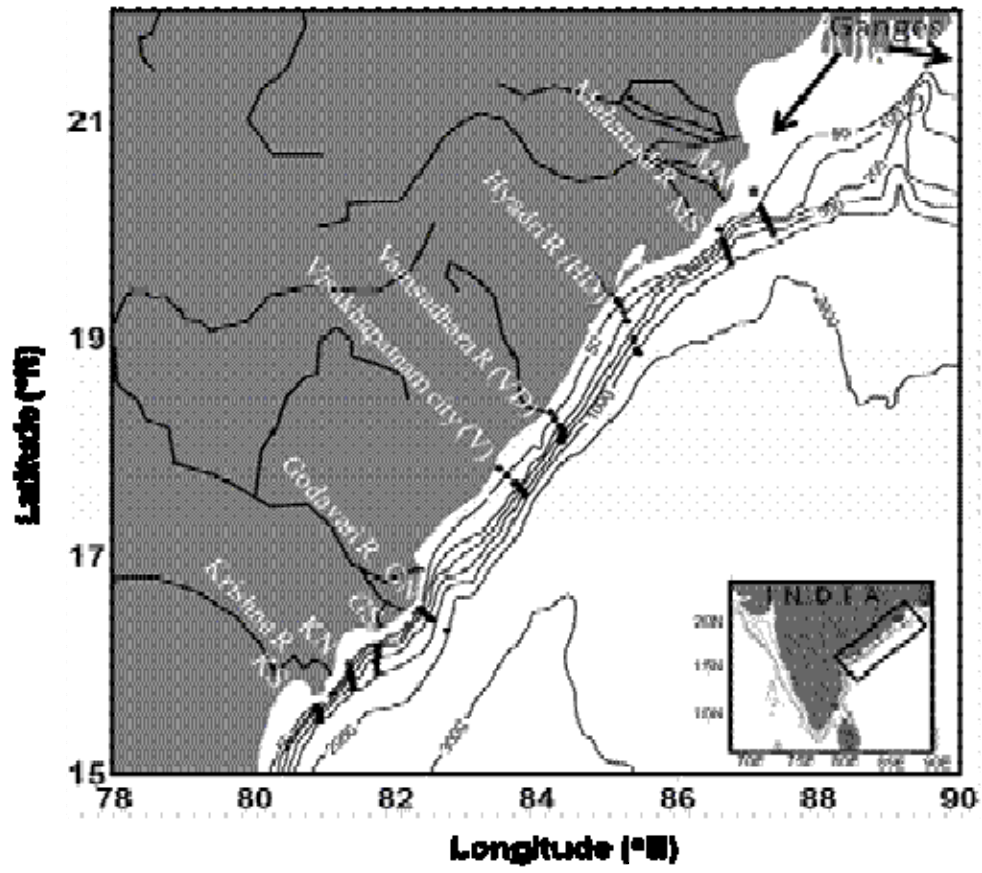


Figure 2.

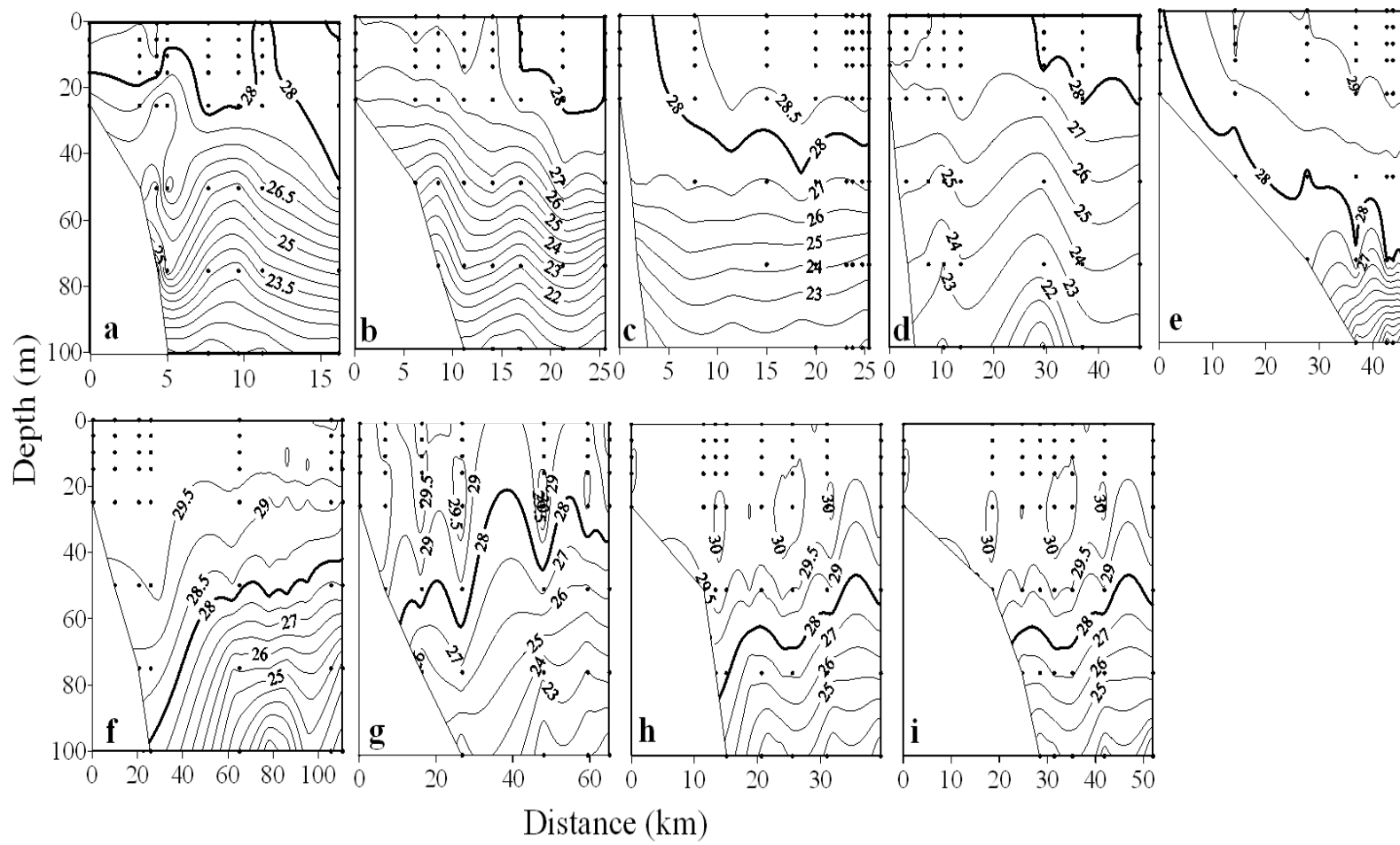


Figure 3:

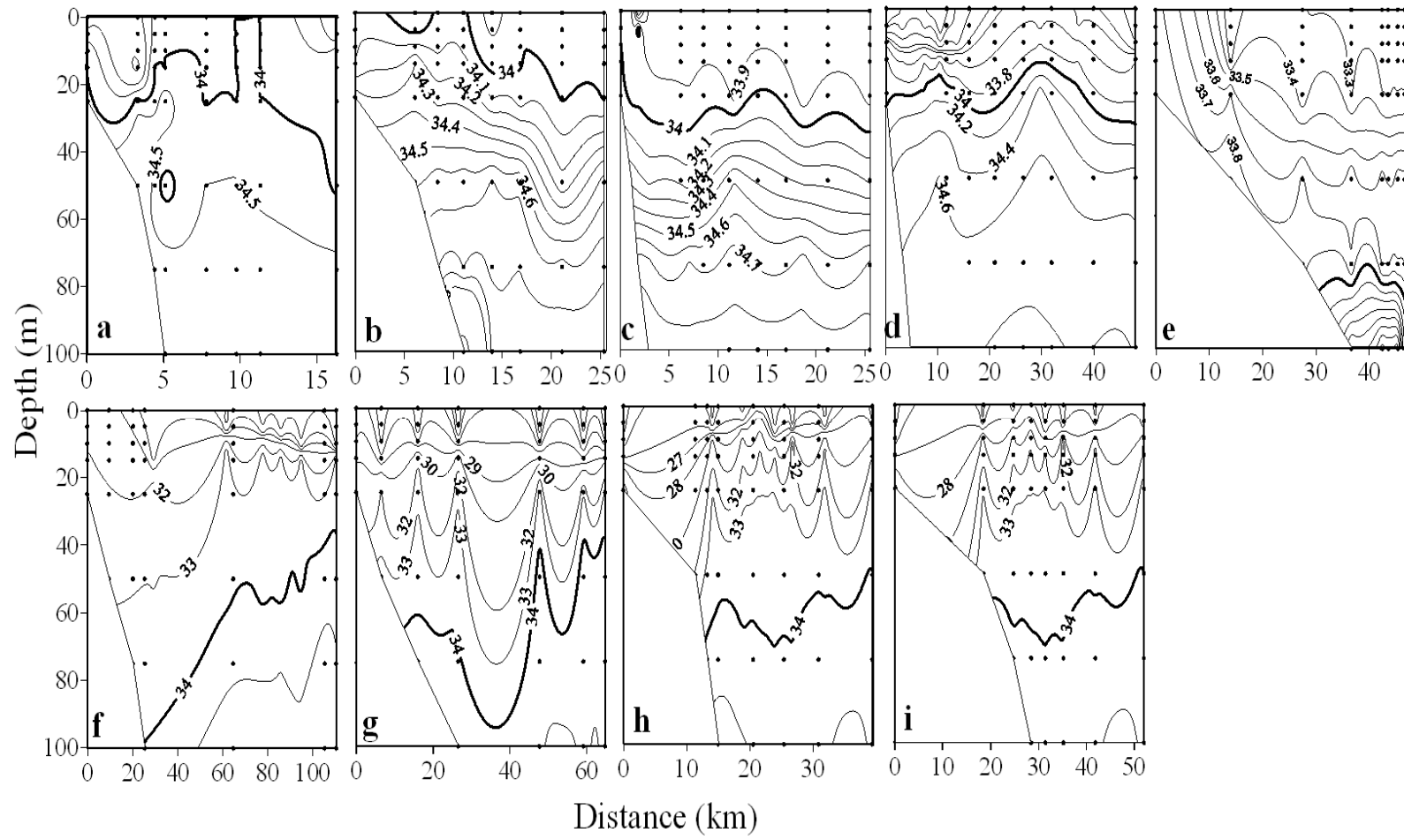


Figure 4:

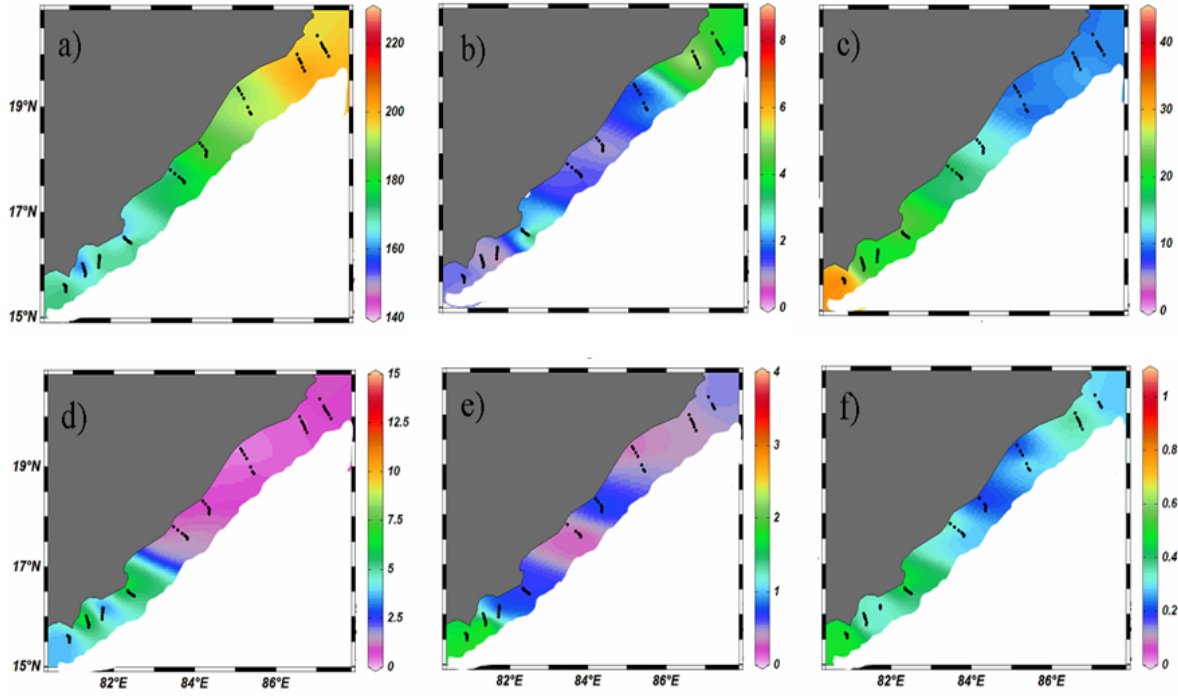


Figure 5:

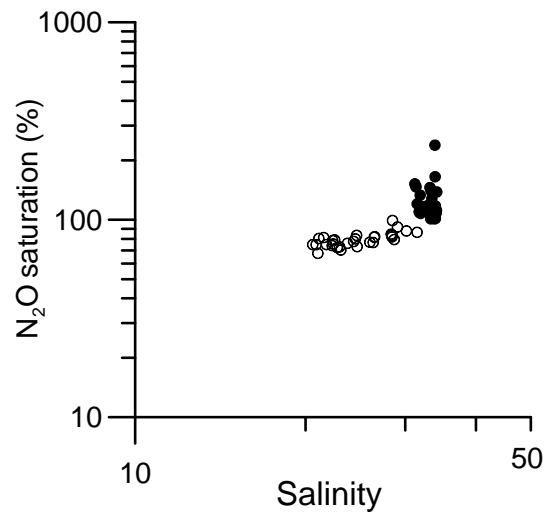


Figure 6.

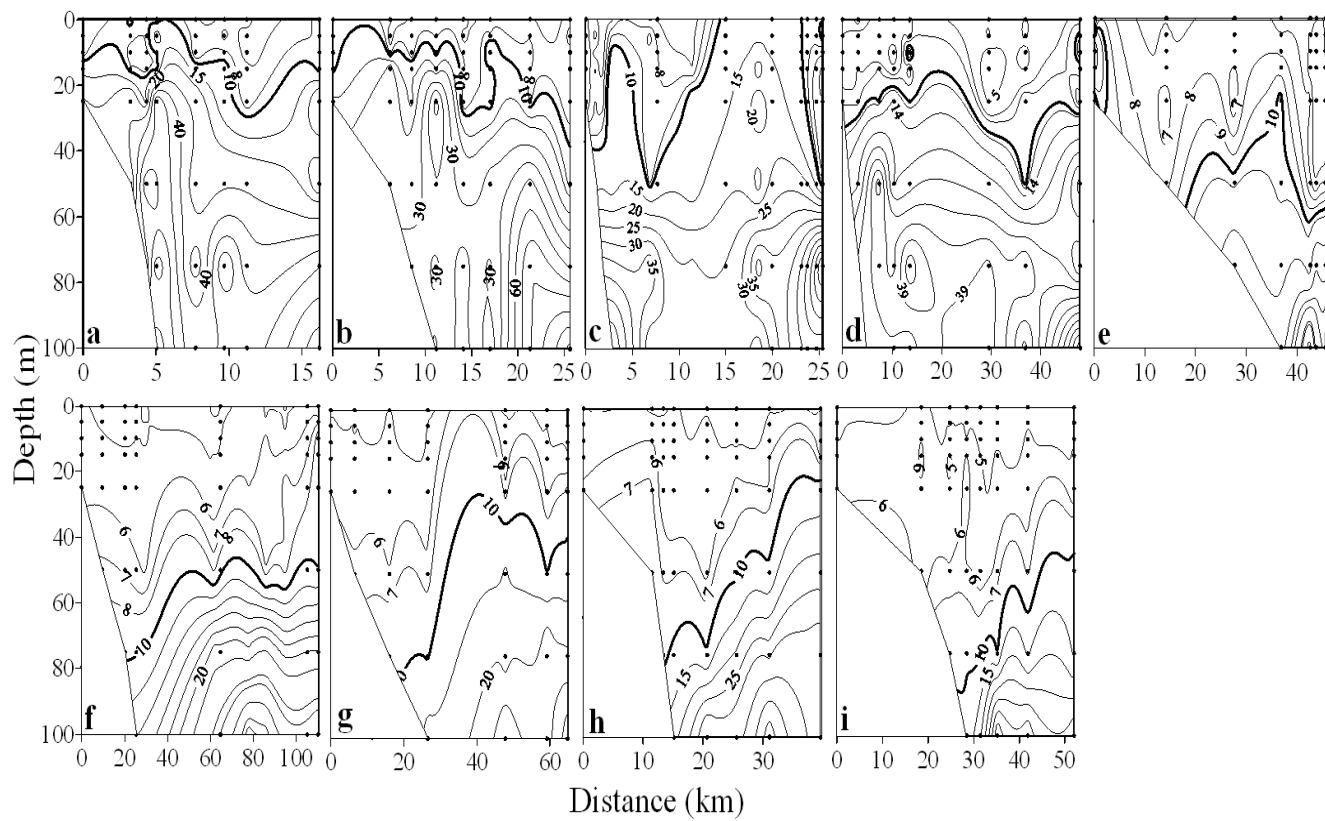


Figure 7:

